ELECTRONICS AND ELECTRICAL ENGINEERING
ISSN 1392-1215 *2006. No. 7(71)*
ELEKTRONIKA IR ELEKTROTECHNIKA

T111 *IMAGE TECHNOLOGY*
VAIZDŲ TECHNOLOGIJA

Image Analysis and Information Fusion Based Defect Detection in Particleboards

J. Guzaitis, A. Verikas

Department of Applied Electronics, Kaunas University of Technology,
Studentų str. 50, LT-51368, Kaunas, Lithuania, phone: 8-687-78621, e-mail.: jonas.guzaitis@ktu.lt

Introduction

A particleboard (sometimes called *chipboard*) is a composite material manufactured from wood particles and a synthetic resin or other suitable binder, which is pressed and extruded. During the production process, defects may appear on board's surface. Image analysis techniques are being increasingly used to automate industrial inspection. However, currently the inspection process still depends mainly on human sight. The nature of this work is very dull and repetitive. Moreover, there could be many human errors in this process. According to some studies, human visual inspection can only catch around 60%–75% of the significant defects [1]. Therefore, to lower the cost of the inspection process and to increase the competitiveness of the products, it is necessary to automate the inspection process.

Most of the available defect detection systems focus on non-textured surfaces such as glass panel [2,3], sheet steel [4], and textile materials [5,6,7,8] using simple thresholding or edge detection techniques. Defects in these images can be easily detected because they commonly have distinctly measured values with respect to those of the uniform background.

Automatic visual inspection techniques for textured images generally compute a set of textural features in the spatial domain or spectral domain, and then search for significant local deviations in the feature values using various classifiers. In the spatial-domain approaches, the commonly used features are the first and second-order statistics derived from the spatial gray-level co-occurrence matrices [9]. However, using this technique it is difficult to locate defect position and separate two defects on the same surface. Another popular method is based on image filtering and simple thresholding. Fourier transform [10,11], Gabor transform [12,13], Wavelet transform [14,15], or low-pass-filtering [10] is usually applied before the thresholding. This technique is rather time consuming but returns more reliable results.

The surface of a particleboard looks like a collection of random gray levels distributed according to the Gaussian law. This type of texture is called statistical and cannot be described using geometrical primitives. The spatial distribution of pixel gray levels is rather stochastic in such a textured image.

In this study, we present an approach to surface defect detection based on fusion of analysis results obtained from several simple techniques.

A low computational time and relatively high defect detection reliability are two characteristic features the technique is aiming at. Before introducing the approach, the statistical characteristics of a fabric texture are examined and some defect examples are described.

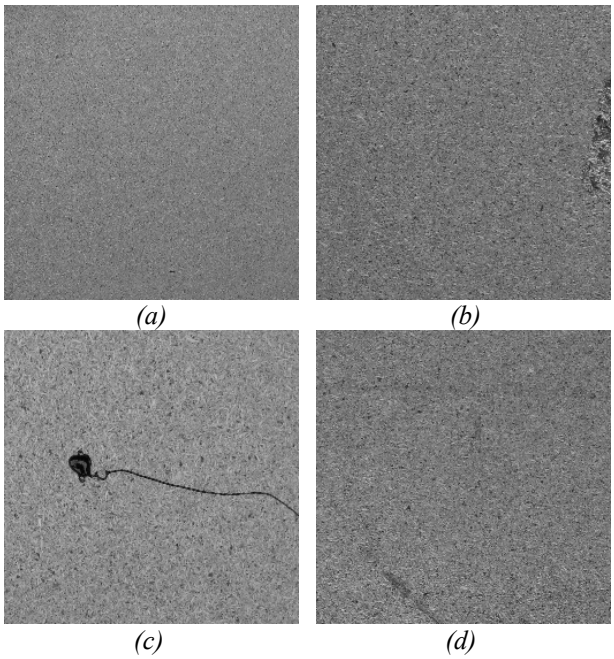

Fig 1. Examples of particleboard surfaces. (a) Quality surface, (b) Hollow near border, (c) Pool of oil, (d) Blot

The subject of research

Particleboards are made of pressed wood particles and a suitable binder. Bigger particles compound the inner

part of the material and smaller ones – the outer surface. This structure makes particleboards strong and smooth. The surface defects may appear during production after smoothing and cutting phases.

The most common defects in particleboards are hollows in surface near the border as shown in Fig. 1 (b). Such defects may occur due to bad trimming after compression or crumbling during transportation. The next class of defects consists of various blots on the surface, Fig. 1 (c,d).

The surface of a particleboard is spotty. It is composed of light and dark speckles – wood particles. The grey level histogram of an image taken from a defect free surface is shown in Fig. 2 (gray line). Three histograms calculated using defective surfaces are drawn in black in Fig. 2. As we can see, there is only a little difference between the distributions.

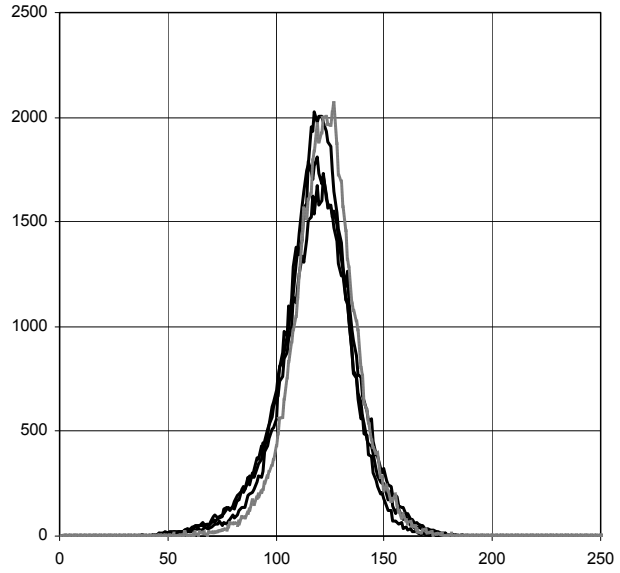

Fig 2. The grey level histograms of three defective (black lines) and one quality (gray line) surfaces

Approach proposed

Image acquisition. Surface hollows are not distinguishable from the background if the light source used is diffusive or directed in parallel to the camera view. This is because the defective and background areas are of the same material and just relief is different. To solve this problem, we use spotlight directed to the surface almost in parallel to a board, as illustrated in Fig. 3. When using such illumination, edges of the hollows make shadows, which are much easer to detect. We have found that the spotlight direction angle α must be in the range from 20° to 30° to obtain good results. Nevertheless, this approach has some drawbacks: small defects make very small shadows; oblique edges make very narrow shadows or even no shadows at all; the shadows are perpendicular to the light direction. Placing several video cameras in sequence along the conveyor with spotlights directed in various directions can solve the last problem. However, in most cases, there is too little space over the conveyor to place bigger diagnostic equipment. Moreover, such an approach is expensive. Because the orientation of most of the defects is parallel or perpendicular to the conveyor belt direction, we propose placing two video cameras with spotlight directed at 45° and 225° to the conveyor belt, respectively. In such a configuration, defects will be visible enough to distinguish them from the background. However, another problem appears when using spotlight, namely the light is unevenly distributed. A surface near spotlight is brighter than on the opposite side. However, normalizing the acquired image against the known background can easily solve this problem.

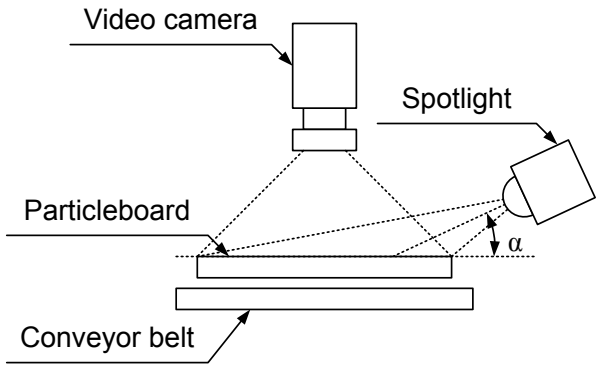

Fig 3. Object lighting scheme

Image processing. To reconcile the contradictory requirements of a high processing speed and relatively high defect detection accuracy, we propose combining results obtained from several simple analysis techniques. The analysis results obtained from the techniques are evaluated by calculating two reliability measures, the global and the local (pixel-wise) one. Values of these measures give an indication of an extent to which we can trust the analysis results. Values of the measures are exploited in the fusion process of the analysis results.

One can expect to solve the problem by simple thresholding applied to low-pass filtered images. However, such a technique is not discriminative enough. As it can be seen from Fig. 2, the grey level histograms computed for the defective and quality surfaces almost completely overlap.

Simple global statistical features such as the mean image intensity, the variance and the median of the intensity, the central moments of the intensity histogram could prove useful for detecting large or numerous defects. However, our experiments performed have shown that for small and sparse defects the discrimination power of such global features is not high enough. Therefore, we resorted to local features in this study.

The local standard deviation of intensity of image pixels is one of such features we consider. Let $(2n+1)\times(2n+1)$ be the size of the window defining the local analysis area. The local standard deviation s_{xy} calculated in the window cantered on the pixel (x, y) is then given by

$$s_{xy} = \sqrt{\frac{1}{(2n+1)^2 - 1} \sum_{i=x-n}^{x+n} \sum_{j=y-n}^{y+n} \left(a_{ij} - \bar{a}_{xy}\right)^2} \,, \qquad (1)$$

where a_{ij} is a gray level of the pixel ij and $\bar{a}_{xy}$ is the mean intensity in the window

$$\bar{a}_{xy} = \frac{1}{(2n+1)^2} \sum_{i=x-n}^{x+n} \sum_{j=y-n}^{y+n} a_{ij} \,. \qquad (2)$$

To eliminate the zero-padding artifacts around the image edges, we used the so-called *border replication*. Using the border replication, the value of any pixel outside the image is determined by replicating the value from the nearest border pixel. To reduce the computation burden the window can be shifted in steps larger than unity.

The "standard deviation image" obtained is then subjected to two types of analysis, the global and the local one. The local analysis is of pixel-wise nature, while the global analysis exploits the discrete probability distribution (the histogram) of the standard deviation random variable.

Global analysis. Let L be the number of grey levels in an image and K_i the number of pixels at a grey level i. The total number of pixels in a given image is then equal to $K = \sum_{i=1}^{L} K_i$ and the probability of a grey level i is defined as

$$p_i = K_i / K \,. \qquad (3)$$

The histogram of an image is given by $h(i) = K_i$.

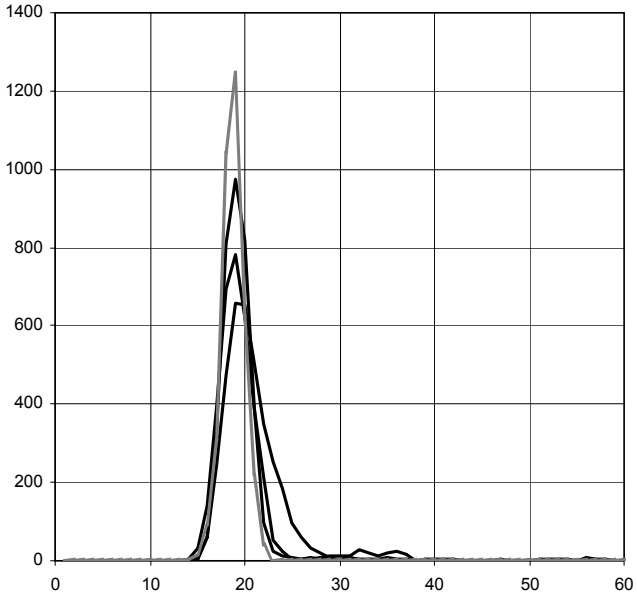

Fig. 4. Histograms calculated using standart deviation images obtained from three defective (black lines) and one quality (gray line) surfaces.

Fig. 4 presents four histograms computed from the standard deviation images. The histogram calculated using a defect free surface is shown in grey. The other three histograms drawn in black were calculated using defective surfaces. As it can be seen from Fig. 4, the histograms calculated using the defective surfaces are more skewed than that obtained from the quality surface.

We use the following features to characterize a histogram.

Variance σ^2

$$\sigma^2 = \sqrt{\sum_{i=1}^{L} (i-m)^2 h(i)} \,, \qquad (4)$$

where m is the mean value

$$m = \sum_{i=1}^{L} h(i) i \,. \qquad (5)$$

Skewness μ_3 is a measure of the asymmetry degree of a histogram around the mean value. The more asymmetric is the histogram, the larger is the skewness vale. A histogram skewed to the left possesses a negative μ_3 value, while a positive μ_3 value is computed for a histogram skewed to the right [16]. Skewness is given by

$$\mu_3 = \sigma^{-3} \sum_{i=1}^{L} (i-m)^3 h(i) \,. \qquad (6)$$

Kurtosis μ_4 (excess kurtosis)

$$\mu_4 = \sigma^{-4} \sum_{i=1}^{L} (i-m)^4 h(i) - 3 \,. \qquad (7)$$

The normal distribution has a kurtosis $\mu_4 = 0$. Positive kurtosis is a sign of a "peaked" distribution while negative kurtosis indicates a "flat" distribution [16].

We expect that a quality surface produces a narrow and sharp histogram exhibiting small skewness and kurtosis values. By contrast, defective surfaces produce non-symmetrical histograms with non-zero skewness and big kurtosis values.

Local Analysis. The local analysis is accomplished by thresholding the standard deviation image and inspecting the obtained result. The standard deviation value is almost the same for any part of a quality surface. However, the standard deviation increases at the edges of local defects. Consequently, we can expect separating the defects from the background by thresholding the standard deviation image. To find the optimal threshold value t^*, we use the standard deviation histogram. As suggested by Otsu [17], the optimal t^* sought is such that the between-cluster variance σ_B^2 is maximized when dividing the histogram into two clusters C_0 and C_1 at the standard deviation value equal to t^*

$$\sigma_B^2(t^*) = \max_{t \in T} \sigma_B^2(t) \,, \qquad (8)$$

where T is a set of the standard deviation values restricted by the boundary values of the histogram. The between-cluster variance is given by

$$\sigma_B^2(t) = P_0(\mu_0 - \mu_T)^2 + P_1(\mu_1 - \mu_T)^2, \qquad (9)$$

where P_0 and P_1 stand for the cluster occurrence probabilities, μ_0 and μ_1 are means of the clusters, and μ_T is the total mean.

Image pixels assigned to the "defects" class during the thresholding are further analyzed. First, the class label of a pixel (x,y) is reversed if $s_{xy} < t^* + \alpha$, where α is a parameter. Next, all the remaining pixels are categorized into connected components. The connected components the size of which $S_{CC} < \lambda$, where λ is a parameter, are eliminated. If after the elimination, the number of remaining connected components is larger than zero, the surface is categorized as "defective".

Decision making. We used a linear discriminant function to make a decision based on features obtained from the global analysis. Let z be a feature vector. The discriminant function $g(\mathrm{z})$ is then given by:

$$g(\mathrm{z}) = w_0 + w_1 z_1 + w_2 z_2 + w_3 z_3, \qquad (10)$$

where z_1 stands for variance, z_2 denotes skewness and z_3 stands for kurtosis. A given surface characterized by a feature vector z is categorized as being a quality surface if $g(\mathrm{z}) > 0$ and as a defective surface otherwise. The optimal values of the parameter vector w are found by solving a system of linear equations.

Assessing the reliability of the analysis. A linear discriminate function $g(\mathrm{z})$ divides the feature space into two parts by a hyper-plane. Given a pattern z, the distance $d(\mathrm{z})$ of the pattern from the hyper-plane can be defined as

$$d(\mathrm{z}) = g(\mathrm{z}) / \| \mathrm{w} \|, \qquad (11)$$

where $\|.\|$ stands for the vector norm. We exploit this distance, to assess the reliability of the global analysis result. The reliability measure $\gamma_G(\mathrm{z})$ is given by

$$\gamma_G(\mathrm{z}) = 1 - \exp\{-\alpha_G \mid d(\mathrm{z}) \mid\}, \qquad (12)$$

where α_G is a parameter chosen experimentally. The $\gamma_G(\mathrm{z})$ measure ranges between 0 and 1. The larger the value, the more reliable is the decision. For a feature vector z lying on the separating hyper-plane, $\gamma_G(\mathrm{z}) = 0$.

To assess the reliability of the local analysis, the between-cluster variance $\sigma_B^2(t^*)$ is exploited. The measure used to assess the reliability of the local analysis result is defined as:

$$\gamma_L(\mathrm{z}) = 1 - \exp\{-\alpha_L \sigma_B^2(t^*)\}, \qquad (13)$$

where the experimentally chosen parameter α_L determines the sensitivity of the measure. The measure also ranges between 0 and 1. The overall reliability measure is then given by

$$\gamma(\mathrm{z}) = \beta\gamma_G(\mathrm{z}) + (1-\beta)\gamma_L(\mathrm{z}), \qquad (14)$$

where the parameter β controls the trade-off between the two parts of the measure. If for a given z, $\gamma(\mathrm{z})$ is less than a predefined threshold, z is assigned to the "rejection" class.

Experiments

Images we used in the experiments were of 256x256 pixels size and $L = 256$ gray levels. All the images were taken by a still photo camera. Twenty quality and twenty defective surfaces were available. Due to the small number of images available, estimation of the correct classification rate obtained from the technique proposed was carried out using the leave-one-out approach. Values of the parameters α, λ, α_G, α_L, and β have been chosen experimentally.

Results

Table 1 summarizes the correct classification rate obtained using the histogram-based features. The table presents the correct classification rate obtained using single features as well as the rate obtained when using all the three features together.

Table 1. The correct classification rate obtained using the histogram-based features

Features	Correct classification rate %
	Quality surfaces
Variance	100
Skewness	100
Kurtosis	95
All	100
	Defective surfaces
Variance	100
Skewness	90
Kurtosis	95
All	100

As it can be seen from the table, the discriminant function exploiting only one—variance—feature provides perfect classification. Thus, for the data at hand there is no need to use the other features. However, the size of the data set used in the tests is very small. Thus, when testing the technique on larger sets, the other features could prove useful for solving the task.

Table 2. The correct classification rate obtained using the local analysis

Features	Correct classification rate %
	Quality surfaces
Local analysis	100
	Defective surfaces
Local analysis	90

Table 2 presents the test results obtained based on the local analysis.

As it can be seen from Table 1 and Table 2, the global analysis based categorization is more accurate than the one exploiting the local analysis results.

Fig. 5 illustrates the local analysis results obtained when analyzing images presented in Fig. 1. The images shown in the figure are the thresholded standard deviation images. An image pixel (x, y) for which $s_{xy} < t^* + \alpha$ is shown in black in the Fig. 5. The higher the s_{xy} value, the brighter is the pixel in the images.

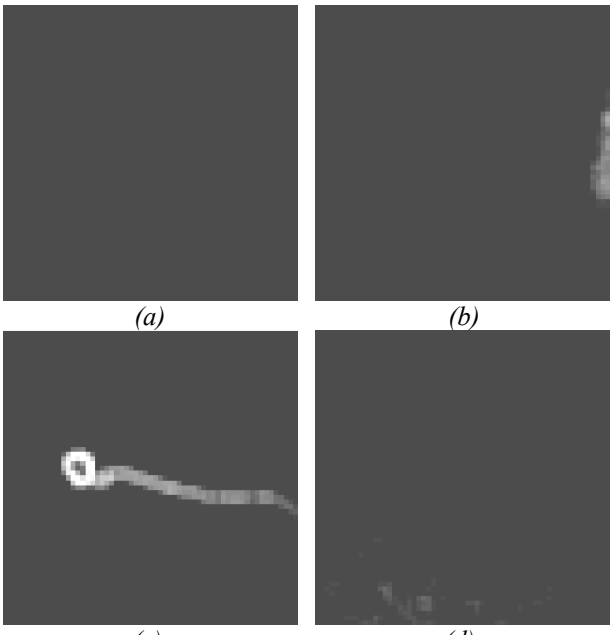

Fig. 5. Thresholded "standard deviation images". (a) Quality surface, (b) Hollow near border, (c) A pool of oil, (d) Blot.

The experimental investigations performed have shown that the technique proposed could detect defects of about 10 times bigger than the average size of a wood particle i. e. defects that are bigger than of about 5-6 mm.

Conclusions

In this paper, we have considered the problem of image analysis based detection of local defects embedded in particleboard surfaces. The focus of the work is defect detection in textured images, rather than classification of defects into various types. The technique is based on analysis of local variance of image intensity values. To achieve reliable defect detection, both local and global analysis are utilized as well as a rejection class is introduced.

The results of the experimental tests performed confirm the efficiency of the technique. The technique is insensitive to lighting changes. It allows detecting both blots and hollows on the particleboard surface. The technique can be applied to detect defects on surfaces that have any *statistical* (non-periodical) texture. However, only a small set of images has been used in the tests. More images will be collected in future studies, especially those containing small-size defects.

References

1. **Schicktanz K.** Automatic fault detection possibilities on nonwoven fabrics, Melliand Textilberichte. – 1993. – No. 74, – P. 294–295.
2. **Ovidiu Ghita, Paul F. Whelan, Tim Carew, Padmapriya Nammalwar**, Quality grading of painted slates using texture analysis // Computers in Industry. – 2005. – No. 56. – P. 802-815.
3. **Tsai Du-Ming, Lin C.-P.** Defect Detection on Gold-Plated Surfaces on PCBs Using Entropy Measures // Advanced Manufacturing Technology. – 2002. – No.20. – P. 420–428.
4. **Pernkopf F.** Detection of surface defects on raw steel blocks using Bayesian network classifiers. //Pattern Analization and Applications. – 2004. – No. 7. – P. 333–342.
5. **Ajay Kumar**, Neural network based detection of local textile defects // Patern Recognition. – 2003. – No. 36. – P. 1645-1659.
6. **Bodnarova A., Bennamoun M., Kubik K. K.** Suitability Analysis of Techniques for Flaw Detection in Textiles using Texture Analysis // Pattern Analysis & Applications. – 2000. – No. 3. – P. 254–266.
7. **Henry Y.T. Nagan, Grantham K.H. Pang, S.P. Yung, Michael K. Ng.** Wavelet based methods on patterned fabric defect detection // Pattern Recognition. – 2005. – No. 38. – P. 559–576.
8. **Tsai D. M., Hsieh C. Y.** Automated surface inspection for directional textures // Image and Vision computing. – 1999. – No. 18. – P. 49–62.
9. **Latif-Amet A., Ertuzun A., Ercil A.** An efficient method for texture defect detection: sub-band domain co-occurrence matrices // Image and Vision computing. – 2000. – No. 18. – P. 543–553.
10. **Du-Ming Tsai, Tse-Yun Huang.** Automated surface inspection for statistical textures // Image and Vision computing. – 2003. – No. 21. – P. 307–323.
11. **Chan C.-H., Pang K. H.** Fabric defect detection by Fourier analysis // IEEE Transactions on Industry Applications. – 2000. – No.36. – P. 1267–1276.
12. **Du-Ming Tsai, C.-P. Lin.** Fast Defect Detection in Textured Surfaces Using 1D Gabor Filtres // Advanced Manufacturing Technology. – 2002. – No.20. – P. 664–675.
13. **Du-Ming Tsai, Ya-Hui Tsai**. Defect detection in textured surfaces using color ring-projection correlation // Machine Vision & Applications. – 2000. – No.13. – P. 194–200;
14. **Henry Y.T. Nagan, Grantham K.H. Pang, S.P. Yung, Michael K. Ng.** Wavelet based methods on patterned fabric defect detection // Pattern Recognition. – 2005. – No. 38. – P. 559–576.
15. **Sungshin Kim, Man Hyung Lee, Kwang-Bang Woo.** Wavelet Analysis to Fabric Defects Detection in Weaving Processes // International Society for Industrial Ecology. – 1999. – No. 3. – P. 1406–1409.
16. **Theodoridis S., Koutroumbas K.** Pattern Recognition, 2nd ed. – San Diego, CA: Academic Press, Inc., 2003.
17. **Verikas A., Malmqvist K., Bergman L.** Detecting and measuring rings in banknote images // Engineering Applications of Artificial Intelligence – 2005. – No. 18. – P. 363–371;

Submitted for publication 2006 05 04

J. Guzaitis, A. Verikas. Image Analysis and Information Fusion Based Defect Detection in Particleboards // Electronics and Electrical Engineering. – Kaunas: Technologija, 2006. – No. 7(71). – P. 67–72.

This paper is concerned with the problem of image analysis based detection of local defects embedded in particleboard surfaces. To increase the defect detection reliability, results obtained from both the global and local image analysis are combined. The Global analysis exploits the discrete probability distribution (the histogram) of the standard deviation of image intensity values. The local analysis is accomplished by thresholding the "standard deviation image" and inspecting the obtained result. The focus of the work is on defect detection in textured images, rather than classification of defects into various types. A 100% correct classification accuracy was obtained when testing the technique proposed on a small set of images. Ill. 5, bibl. 17 (in English; summaries in English, Russian and Lithuanian).

Й. Гузайтис, А. Верикас. Обнаружение дефектов на поверхности ДСП с использованием анализа изображений и совмещения информации // Электроника и электротехника. – Каунас: Технология, 2006. – № 7(71). – С. 67–72.

Расматривается проблемма обнаружения местных дефектов на поверхности ДСП с использованием анализа изображений. Для увеличения надежности обнаружения дефекта, совмещаются результаты глобального и местного анализа. Глобальный анализ оценивает параметры гистограммы стандартного отклонения значений интенсивности пикселей изображения. Местный анализ оценивает каждую точку "изображения стандартного отклонения" отдельно. Главный акцент работы основан на обнаружении дефектов в текстурных изображениях, но не на классификации дефектов на различные типы. При экспериментировании была получена 100% точность классификации на малой выборке изображений. Ил. 5, библ. 17 (на английском языке; рефераты на английском, русском и литовском яз.).

J. Guzaitis, A. Verikas. Vaizdų analize ir informacijos sujungimu grįstas drožlių plokščių paviršinių defektų aptikimas // Elektronika ir elektrotechnika. – Kaunas: Technologija, 2006. – Nr. 7(71). – P. 67–72.

Siūlomas vaizdų analize grįstas drožlių plokščių paviršinių defektų aptikimo būdas, jungiantis globalios ir lokalios vaizdų analizės rezultatus. Globalios analizės metu apskaičiuojami vaizdo pikselių intensyvumo vidutinio kvadratinio nuokrypio histogramą apibūdinantys parametrai. Lokali analizė atskirai vertina kiekvieną „vidutinio kvadratinio nuokrypio vaizdo" tašką. Daugiausia dėmesio skiriama defektų aptikimui margame paviršiuje, o ne defektų klasifikavimui į atskiras rūšis. Atliekant eksperimentus su palyginti maža vaizdų imtimi, visi šios imties vaizdai buvo klasifikuoti teisingai. Il. 5, bibl. 17 (anglų kalba; santraukos anglų, rusų ir lietuvių k.).